$$\alpha = 53.7°$$
$$\beta = 50.7°$$

CP basis forms: *TF basis forms:*

$q_2 = 0.075 Å$ $F_{CP} = 0.1°$ $\Phi_2 = 3.4°$ $P_2 = 214°$
$q_3 = 0.647 Å$ $\Phi_3 = 59.3°$

Figure 6. Interplanar angles (α, β) in the thiane ring observed[40] for *trans*-2-methylthiane-1-(*p*-tosyl)imide, indicating the flattening of the ring at the C–S–C apex. Lower part shows the basis forms that are part of the linear combinations prescribed by the CP (left) and TF (right) formalisms, respectively.

combination of the $^{S,4}B$ and the $^{S}C_4$ form, whereas the TF formalism takes it to be a combination of $B_{S,4}$ and $^{S}C_4$ forms. Again, based on the internal angular characteristics of the ring (the C–S–C apex less puckered than the C–C_4–C apex), one is inclined to prefer the TF interpretation. However, it should be stressed that from a mathematical point of view the CP interpretation is

correct. The discrepancies noted above stem from the difference in reference systems used by the two methods: the CP formalism employs an external reference plane, whereas the TF formalism is based on internal coordinates only. The examples given above just demonstrate the hazards inherent in using externally referenced puckering coordinates to interpret the internal angular characteristics of a six-membered ring.

Conclusion

The TF formalism delineated by eq 10 gives a description of six-membered ring conformations in terms of three ring puckering coordinates derived from the endocyclic torsion angles. As such, it relies solely on internal coordinates and is therefore not in need of an external reference plane, e.g., the mean plane in the CP formalism. This is an important feature since the determination of a reference plane requires the Cartesian coordinates of *all* ring atoms to be known which consequently makes it virtually impossible to apply the CP formalism to molecules in solution. Conversely, the TF formalism is in a sense geared to dealing with six-membered rings in solution as it utilizes torsion angle magnitudes which may be derived from NMR coupling constants. Especially with respect to the latter type of work, it is noted that the linear equation system given by eq 10 can still be solved for the three ring puckering coordinates if only three torsions are known. Admittedly, the TF formalism lacks the CP formalism's exactness, but its accuracy seems satisfactory for all practical purposes. More important, especially in nonequilateral rings, the TF method appears to be consistent with internal angular characteristics of rings such as local flattening, etc. It is for these reasons that the TF formalism may well serve existing stereochemical needs.

Kinetic Models for Gas-Phase Electron-Transfer Reactions between Nitrobenzenes

Chau-Chung Han, James L. Wilbur, and John I. Brauman*

Contribution from the Department of Chemistry, Stanford University, Stanford, California 94305-5080. Received June 3, 1991

Abstract: Rate constants for gas-phase electron-transfer reactions between substituted nitrobenzenes have been measured using ion cyclotron resonance spectroscopy. On the basis of the assumption that these reactions occur through the formation of an intermediate complex, a statistical model is used to interpret the reaction kinetics. The intersecting parabolas quantum mechanical model provides an alternative description of the energy surface. Energy barriers are found to be consistent for the two methods. The results for exothermic reactions are consistent with a Marcus theory analysis, but suggest that a zero-order potential energy surface may not be completely adequate for quantitative prediction of reaction rates.

Introduction

Electron-transfer reactions have long been studied in both solution and gas phases. In solution, they generally have an activation barrier that can be ascribed to structural deformation of the reactants (the inner-sphere reorganization energy) and the reorientation of solvent dipoles (the outer-sphere reorganization energy) upon the formation of the transition state. Early gas-phase studies mostly concentrated on reactions between rare gas cations or diatomic cations and small molecules (2–3 atoms) that had no analogous reactions in solution. Recently, systematic studies on

gas-phase electron-transfer reactions of metallocenes[1] and nitrobenzenes[2] which had been studied in solution phase have appeared.

Kinetics of gas-phase electron-transfer reactions are governed by, among other things, energy defects and Franck–Condon factors of the reacting pair.[3] At thermal energies the energy resonance

(1) (a) Richardson, D. E. *J. Phys. Chem.* **1986**, *90*, 3697. (b) Eyler, J. R.; Richardson, D. E. *J. Am. Chem. Soc.* **1985**, *107*, 6130. (c) Phelps, D. K.; Gord, James, R.; Freiser, B. S.; Weaver, M. J. *J. Phys. Chem.* **1991**, *95*, 4338.
(2) Grimsrud, E. P.; Caldwell, G.; Chowdhury, S.; Kebarle, P. *J. Am. Chem. Soc.* **1985**, *107*, 4627.

condition is generally more important,[3b,f,g] because the Franck–Condon manifold is likely to be distorted[4] due to interactions between the slowly moving reactants that result in polarization or deformation of the neutral molecule.[3d,5] The long lifetime of the collision complex allows the reactants to experience a wide range of geometries so that optical Franck–Condon factors are not appropriate for these low impact energy electron-transfer reactions.[6–8] At high collision energies the Franck–Condon factor becomes more important[3f,g] because the interaction time is reduced, due to faster relative motion, with the result that nuclear reorganization does not occur during an encounter. In addition, the increased kinetic energy can be converted into internal energy[3e,9] so that endothermic reaction channels can be accessed.

In studies of gas-phase collisional quenching of vibrationally excited ions, it has been found that the efficiency is often high when the quencher is the parent neutral,[10,11] and it has been suggested that resonant electron transfer provides a very efficient mechanism for energy relaxation.[12] Direct comparisons of the dynamics of electron transfer and collisional quenching, however, are scarce.[11a]

Gas-phase electron-transfer reactions with favorable Franck–Condon factors and small energy defects generally proceed very rapidly. When a reaction occurs at a rate faster than the collision rate, long-distance electron jump has been commonly invoked. However, long-distance electron jump has been unequivocally identified only for a small number of reactions involving small cations and neutral reactants. An early theoretical study concluded that thermal energy, long-distance electron transfer should only occur in systems with spherically symmetric interaction potentials with some specially aligned homonuclear diatomics as the only exceptions.[13] While most exothermic gas-phase electron-transfer reactions proceed at near the collision rate, examples exist where high activation barriers arising from large geometry changes upon electron transfer retard reaction rates significantly.[1,14,15]

Kinetics of electron-transfer reactions involving nitroaromatics in aqueous solution were recently reported.[16] These solution reactions have an activation energy of 3–6 kcal/mol, which was ascribed mainly to solvent reorganization; rate constants for degenerate electron-transfer reactions of differently substituted nitrobenzenes were found to be in the range of 10^5–10^8 M^{-1} s^{-1}.

In this paper, we report the kinetics of electron-transfer reactions between nitrobenzenes in the gas phase. Two models are used to help in the interpretation of the rate constants. A statistical model that has been applied previously to gas-phase atom- and group-transfer reactions relates the rate constants to the energy surface. This is compared with a semiempirical quantum mechanical (MNDO) calculation which estimates the distortion energy required for electron transfer.

Experimental Section

All chemicals used in this study were obtained from commercial sources. Liquid samples were purified by gas chromatography, and solid samples were purified by either vacuum distillation or sublimation. All samples were degassed by several freeze–pump–thaw cycles on the ion cyclotron resonance foreline before being leaked into the high-vacuum ion trap.

A pulsed ion cyclotron resonance spectrometer (ICR) equipped with a rectangular cell (1 × 1 × 1.5 in.), a 9-in.-diameter electromagnet (Varian V-3400, operated at 1.2–1.3 T), and a capacitance bridge detector was used for the generation, storage, and mass analysis of the ionic species involved. The pulse sequence and data management routines were controlled by an IBM-PC. The intrinsic time resolution is 1 ms, but the 8-ms-wide detect pulse determined our time resolution. The detection (ca. 200-mV P-P) and double resonance (0.5–2-V P-P) signals were provided by separate frequency synthesizers (Hewlett-Packard 3325A and Wavetek 171, respectively).

Some of these reactions were also studied using an Ion-Spec FTMS-2000 controlled by a Wells American (A-Star PC/AT compatible) computer and configured with impulse excitation. Other experimental details were similar.

Reactant radical anions were generated by attachment of thermal electrons to parent molecules. For a reaction mixture composed of two nitrobenzenes, designated by A and B, both A$^-$ and B$^-$ are formed in the initial ionizing electron beam pulse. Their relative abundances are determined by their partial pressures, the electron capture cross sections, and the lifetimes of the incipient parent radical anions which, in turn, are largely determined by the stabilities (i.e., electron affinities) and molecular complexity of the parent molecules. In order to generate sufficient amounts of the reactant anions, trapped thermal electrons were not ejected until 20–50 ms after the electron beam pulse. Electrons were then ejected by applying a 11–13-MHz signal to the trapping plates.

The electron transfer reactions studied in the energetically accessible direction are represented as eq 1. In exothermic reactions it is the product anion, B$^-$, that is easier to form in the initial ionizing electron capture process. Therefore, an excess of A is needed in order to build

$$A^- + B \rightarrow A + B^- \tag{1}$$

up enough abundances of A$^-$ at the initial ionization stage. Typically, $P_A = (0.4–1.6) \times 10^{-6}$ Torr and $P_B = (0.4–4) \times 10^{-7}$ Torr were used. These pressure readings were ionization gauge (Varian 844) values calibrated against a capacitance manometer (MKS 170 Baratron with a 315BH-1 head). Calibration was carried out daily at the end of the kinetic runs for each electron acceptor.

The temporal pseudo-first-order exponential decay of A$^-$ was monitored and signal averaged 10–30 times at each constant-incremental time delay with respect to the electron beam pulse. At each time delay, the resonance maximum was located by sweeping the radiofrequency signal generator across the peak to obtain the strongest signal reading before they were stored and processed. Possible resonance shifts due to changes in space-charge distribution are thus corrected. Typically, the decaying A$^-$ signal was recorded for $3\frac{1}{2}$–5 half-lives while the product ion, B$^-$, was continuously removed from the ion trap by double resonance ion ejection. The ion signal intensities were displayed in a semilog fashion, so that an exponential decay appears as a linear function of time ensuring that nonexponential decay of A$^-$ could be detected. The slope of such a linear semilog plot (typically consisting of 10–15 equally spaced points), which after correction has been made for unreactive ion loss, is equated with the pseudo-first-order reaction rate constant. In view of the long exponential decay observed, we do not consider energized ion reactions to be a problem.

The kinetics of the two degenerate exchange reactions (nitrobenzene(–) + nitrobenzene; 3-chloronitrobenzene(–) + 3-chloronitrobenzene) and the exothermic nitrobenzene(–) + 3-chloronitrobenzene reaction were also carried out using the Fourier transform system. In these experiments, all of the ions are detected simultaneously, and there

(3) (a) Laudenslager, J. B.; Huntress, W. T., Jr.; Bowers, M. T. *J. Chem. Phys.* **1974**, *61*, 4600. (b) Anicich, V. G.; Laudenslager, J. B.; Huntress, W. T., Jr.; Futrell, J. H. *J. Chem. Phys.* **1977**, *67*, 4340. (c) Bearman, G. H.; Harris, H. H.; Leventhal, J. J. *J. Chem. Phys.* **1977**, *66*, 4111. (d) Chau, M.; Bowers, M. T. *Chem. Phys. Lett.* **1976**, *44*, 490. (e) Flannery, M. R.; Cosby, P. C.; Moran, T. F. *J. Chem. Phys.* **1973**, *59*, 5494. (f) Moran, T. F.; Flannery, M. R.; Cosby, P. C. *J. Chem. Phys.* **1973**, *61*, 1261. (g) Hedrick, A. F.; Moran, T. F.; McCann, K. J.; Flannery, M. R. *J. Chem. Phys.* **1977**, *66*, 24. (h) Lee, C.-Y.; DePristo, A. E. *J. Chem. Phys.* **1984**, *81*, 3512.

(4) (a) Marx, R. In *Ionic Processes in the Gas Phase*; Ferreira, M. A. A., Ed.; Reidel: Boston, 1984; p 67. (b) Marx, R. In *Kinetics of Ion–Molecule Reactions*; Ausloos, P., Ed.; Plenum: New York, 1978; p 103. (c) Govers, T. R.; Gerard, M.; Marx, R. *Chem. Phys.* **1977**, *23*, 411. (d) Lipeles, M. *J. Chem. Phys.* **1969**, *51*, 1252.

(5) (a) Ausloos, P.; Eyler, J. R.; Lias, S. G. *Chem. Phys. Lett.* **1975**, *30*, 21. (b) McMillan, M. R.; Coplan, M. A. *J. Chem. Phys.* **1979**, *71*, 3063.

(6) Gauglhofer, I.; Kevan, L. *Chem. Phys. Lett.* **1972**, *16*, 492.

(7) Jówko, A.; Forys, M.; Jonsson, B. Ö. *Int. J. Mass Spectrom. Ion Phys.* **1979**, *29*, 249.

(8) (a) Marx, R.; Mauclaire, G.; Derai, R. *Int. J. Mass Spectrom. Ion Phys.* **1983**, *47*, 155. (b) Derai, R.; Mauclaire, G.; Marx, R. *Chem. Phys. Lett.* **1982**, *86*, 275. (c) Derai, R.; Fenistein, S.; Gerard-Ain, M.; Govers, T. R.; Marx, R.; Mauclaire, G.; Profous, C. Z.; Sourisseau, C. *Chem. Phys.* **1979**, *44*, 65.

(9) However, there exists an example where ion kinetic energy does not seem to be effectively converted into internal (electronic) energy. See ref 3c.

(10) Wight, C. A.; Beauchamp, J. L. *J. Phys. Chem.* **1984**, *88*, 4426.

(11) (a) Barfknecht, A. T.; Brauman, J. I. *J. Chem. Phys.* **1986**, *84*, 3870. (b) Ferguson, E. E. In *Swarms of Ions and Electrons in Gases*; Lindinger, W., Mark, T. D., Howorka, F., Eds.; Springer: Vienna, 1984. (c) Kim, M. S.; Dunbar, R. C. *Chem. Phys. Lett.* **1979**, *60*, 247. (d) Orlowski, E.; Freiser, B. S.; Beauchamp, J. L. *Chem. Phys.* **1977**, *16*, 439.

(12) McMahon, T. B.; Miasek, P. G.; Beauchamp, J. L. *Int. J. Mass Spectrom. Ion Phys.* **1976**, *21*, 63.

(13) Bates, D. R.; Lynn, N. *Proc. R. Soc. London, A* **1959**, *253*, 141.

(14) (a) Grimsrud, E. P.; Chowdhury, S.; Kebarle, P. *J. Chem. Phys.* **1985**, *83*, 1059. (b) Drzaic, P. S.; Brauman, J. I. *J. Am. Chem. Soc.* **1982**, *104*, 13 and references cited therein.

(15) (a) Nelsen, S. F.; Rumack, D. T.; Meot-Ner, M. *J. Am. Chem. Soc.* **1987**, *109*, 1373. (b) Richardson, D. E.; Christ, C.; Sharpe, P.; Eyler, J. R. *J. Am. Chem. Soc.* **1987**, *109*, 3894.

(16) Meot-Ner, M.; Neta, N. *J. Phys. Chem.* **1986**, *90*, 4648.

Electron-Transfer Reactions between Nitrobenzenes

J. Am. Chem. Soc., Vol. 114, No. 3, 1992 889

Table I. Electron-Transfer Rate Constants, Reaction Efficiencies, Reaction Energetics, and E_{diff} for $C_6H_4XNO_2^- + C_6H_4YNO_2 \rightarrow$ $C_6H_4YNO_2^- + C_6H_4XNO_2$

X	Y	$k_2{}^a$	efficiency^b	$-\Delta H^{\circ}{}_{rxn}{}^c$	$-E_{dif}{}^d$
H	$D_5{}^e$	3.7 ± 0.7	0.17 ± 0.03	~0	10.1 ± 0.4^f
$D_5{}^e$	H	2.7 ± 0.3	0.12 ± 0.02	~0	
H	4-F	5.6 ± 0.9	0.34 ± 0.05	2.2	11.0 ± 0.5
H	3-F	14 ± 2	0.78 ± 0.11	5.2	14.7 ± 1.0
H	3-Cl	17.4 ± 0.5	0.90 ± 0.03	6.0	
3-Cl	3-Cl	3.5 ± 0.8	0.19 ± 0.04	~0	12.1 ± 0.5
3-F	3-Cl	14 ± 1	0.74 ± 0.05	0.8	≥15.1 ± 0.4^g
4-F	3-Cl	17.7 ± 0.5	0.95 ± 0.03	3.8	

$^a k_2$, the experimental second-order reaction rate constant, expressed in units of 10^{-10} cm^3 molecule^{-1} s^{-1} and measured at ambient temperature of 350 K. The uncertainties reflect the reproducibility on 2–4 different days and repesent one standard deviation of the results. ^{b} Reaction efficiency = k_2/k_{ADO} where k_{ADO} is the theoretical ion-molecule collision rate constant predicted by the average dipole orientation (ADO) theory; see ref 19. ^{c} kcal/mol; data from ref 2. $^d E_{diff}$, the energy difference between the electron-transfer transition state and the orbiting transition state obtained by RRKM simulation. The uncertainty reflects the error bar in the experimental reaction efficiency. ^{e} Perdeuteriated nitrobenzene. ^{f} Obtained with appropriate vibrational frequencies of both the protio and deuterio molecules as well as the corresponding anions in the RRKM calculations. The vibrational frequencies are based on those reported in refs 34 and 35. ^{g} Obtained with the approximation that efficiency = BF; see text.

are no complications from, and thus no corrections for, possible resonance shifts.

The contribution from unreactive ion loss to the measured total ion decay rate constant is accounted for when the experimental pseudo-first-order rate constant, k_{OBS}, is converted[17] into the second-order reaction rate constant, k_2, according to Scheme I. Unreactive ion-loss rate

Scheme I

$$I_t(A^-) = I_o(A^-) \exp(-k_{OBS}t)$$

$$k_{OBS} = k_{IL}(A^-) + k_2[B]$$

$$k_2 = \frac{k_{OBS} - k_{IL}(A^-)}{[B]}$$
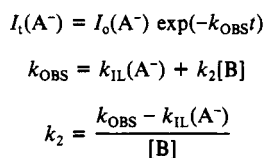
constants were measured without applying double resonance ion ejection. For a thermoneutral reaction where the ion signal of A^- has significant intensity at equilibrium, the decay of A^- due to unreactive ion loss was monitored directly. For an exothermic reaction, the pseudo-first-order unreactive ion-loss rate constant of B^-, $k_{IL}(B^-)$, was obtained by monitoring the decay of B^- after all the A^- had reacted or after reaction 1 had reached equilibrium. The pseudo-first-order ion-loss rate constant for A^-, $k_{IL}(A^-)$, was then estimated from $k_{IL}(B^-)$ using[18] eq 2, where P_A and P_B represent the partial pressures of A and B, respectively, and μ_{BA} etc. are the reduced masses of the corresponding colliding ion–neutral pairs.

$$\frac{k_{IL}(A^-)}{k_{IL}(B^-)} = \frac{1}{P_A + P_B} \frac{(M_A)^{1/2}}{(M_B)^{1/2}} \left\{ P_A \frac{(\mu_{BA})^{1/2}}{(\mu_{AA})^{1/2}} + P_B \frac{(\mu_{BB})^{1/2}}{(\mu_{AB})^{1/2}} \right\} \quad (2)$$

The combined uncertainty in pressure and pseudo-first-order reaction rate constant determinations is estimated at ~20% for each daily result. The reproducibility of a given reaction on different days was generally better than 20%.

Results

Eight rate constants for electron-transfer reactions between substituted nitrobenzenes (NB = nitrobenzene, XNB = substituted nitrobenzene) are summarized in Table I. Three of them are quasi-degenerate reactions where isotopic labels were used to distinguish the reactant ion from the product. All reactions are

Figure 1. Double-well potential energy curve for gas-phase ion–molecule reactions. E_W and E_{dif} as shown have negative values.

fast; however, the degenerate reactions are clearly not collision limited. The error limits in Table I are based on the reproducibility of our measurements. The accuracy of these values is probably less, but the reaction efficiencies—the fraction of orbiting collisions[19] leading to reaction—are all less than unity. Due to the combined uncertainty in our experimental results and calculated collision rates,[19] we do not attempt to ascribe the slightly different reaction efficiencies measured for the degenerate reactions of $NB^{-/0}$ in the opposite directions (first two entries) to isotope effects.

Discussion

The results shown in Table I indicate that electron transfer between nitrobenzenes is quite efficient but clearly less than collision limited when the reaction lacks thermodynamic driving force. Our results are consistent with those obtained by high-pressure mass spectrometry for analogous but more exothermic reactions,[2] $-\Delta H^{\circ}{}_{rxn}$ = 8.8–21.5 kcal/mol, whose reaction efficiencies range from 1 to 1.3.

In general, the statistical limit to reaction efficiency of a thermoneutral ion–molecule reaction that proceeds through the formation of a long-lived intermediate complex is 0.5. This would be the case if the reaction dynamics are governed by a single-well potential energy surface. For thermoneutral reactions occurring on a double-well (or more complicated) potential energy surface, the reaction efficiencies will be less than 0.5 unless interconversion between reactant- and product-like complexes occurs many times before the reaction complex decomposes.

Since the initial proposal that a double-well (and more complicated) potential energy surface model can rationalize many observed slow gas-phase ion–molecule reactions,[20a] this proposal has been widely adopted. This model, Figure 1, originally applied to group[20] and proton[21a] transfer reactions, has been applied to interpret gas-phase electron-transfer reaction kinetics.[1,14a]

The reaction efficiencies for the two quasi-degenerate electron exchange reactions, $NB^{-/0}$ and 3-ClNB$^{-/0}$, are both ~0.2. For the reactions reported here, the spin multiplicity is conserved and reaction efficiency smoothly increases with increasing thermodynamic driving force. These together suggest that the slowness of the (near) thermoneutral reactions is due to the presence of energy barriers[22] along the reaction coordinate, and a double-well

(17) Unreactive ion loss is a nearly first-order process at low pressures (being a very weak function of pressure) and becomes second-order at higher pressures; see: Farneth, W. E. Ph.D. Thesis, Stanford University, Stanford, CA, 1975. At a given pressure the kinetics of unreactive ion loss can be characterized by a pseudo-first-order rate constant k_{IL}.
(18) This is based on an equation derived by Olmstead; see: Olmstead, W. N. Ph.D. Thesis, Stanford University, Stanford, CA, 1978, pp 95–100.
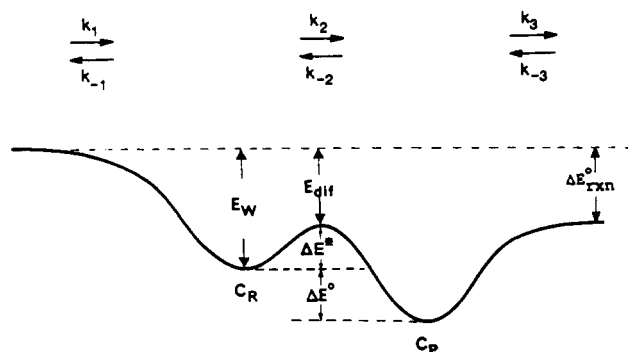
(19) Su, T.; Bowers, M. T. In *Gas Phase Ion Chemistry*; Bowers, M. T., Ed.; Academic Press: New York, 1979; Vol. 1, Chapter 3. The more recent analysis of Su and Chesnavich (Su, T.; Chesnavich, W. J. *J. Chem. Phys.* **1982**, *76*, 5183) gives rate constants which are typically about 20% faster for systems with large dipole moments. This would make our efficiencies somewhat lower and the barriers somewhat higher, but the quantitative differences would not be significant.
(20) (a) Olmstead, W. N.; Brauman, J. I. *J. Am. Chem. Soc.* **1977**, *99*, 4219. (b) Asubiojo, O. I.; Brauman, J. I. *J. Am. Chem. Soc.* **1979**, *101*, 3715.
(21) (a) Farneth, W. E.; Brauman, J. I. *J. Am. Chem. Soc.* **1976**, *98*, 7891. (b) Dodd, J. A.; Baer, S.; Moylan, C. R.; Brauman, J. I. *J. Am. Chem. Soc.* **1991**, *113*, 5942. (c) Lim, K. F.; Brauman, J. I. *J. Chem. Phys.* **1991**, *94*, 7146.
(22) Slow gas-phase electron-transfer reactions can also be attributed to nonadiabaticity arising from a change of electron spin state upon electron transfer. This has been suggested[1] as a possible cause of the extremely slow $Cp_2Mn^{+/0}$ (Cp = cyclopentadienyl) electron exchange. For electron-transfer reactions between nitrobenzenes, no change in electron spin is involved.

potential energy surface is a reasonable model for the description of the kinetics studied. Since the equilibrium geometries of the neutral molecule and the radical anion are expected to be somewhat different, the energy barriers may arise from deformation of reactant molecules upon the formation of the transition state. Retardation of electron transfer due to large geometry changes upon reaction has been noted for several systems.[1,14,15] From the ~20% reaction efficiencies of the thermoneutral reactions and the large acceleration effect of reaction exothermicity on reaction rates, the intrinsic activation barrier due to molecular reorganization is expected to be small.

While the double-well potential energy surface model has been applied to slow gas-phase electron-transfer reactions, little information on reaction dynamics has been obtained for this model. We attempt to obtain quantitative information on the barriers so as to test the rate–equilibrium relationship and probe the nature of gas-phase electron-transfer reactions.

Statistical Model. We utilize the statistical model that has been successfully applied to gas-phase proton- and group-transfer reactions which share the same double-well potential energy surface as the electron-transfer reactions.[20,21a] A statistical treatment has been applied to the analysis of autodetachment lifetimes of molecular anions formed in an electronic scattering process.[23] Before we apply a statistical treatment to electron-transfer reactions, however, we need to justify the exclusion of several conditions that may preclude using such a model. These include the possibility of electron tunneling and long-distance electron transfer (without formation of collision complex on the double-well surface). We have recently shown that some slightly slow reactions can be a consequence of other, dynamic factors,[21b,c] but we postulate that such effects are not the important factor in the reactions discussed here.

Since the ion–molecule collision complex is chemically activated under our experimental conditions due to the lack of an efficient relaxation mechanism, and since the electron-transfer transition state is lower in energy than the reactants, electron tunneling is unlikely to play a significant role in these gas-phase electron-transfer reactions. Similar arguments may also apply to (secondary) kinetic isotope effects, which may affect the measured rates for the two degenerate reactions studied. While long-distance electron jump has been identified in some, mostly small, cationic systems, it is likely to be important only when the ion–molecule interaction potential has spherical symmetry.[13] Although high-order perturbations in these large, diffuse nitrobenzene anions may relax the quantum mechanical criterion about the symmetry of the interaction potential somewhat, we do not expect to have a noticeable contribution from the long-distance electron-transfer mechanism to our reaction kinetics.

In addition, we further assumed that electron transfer only occurs at the isoenergetic nuclear configuration.[24a] As such, the reaction coordinate for electron-transfer reactions is defined by some nuclear coordinates so that they are formally identical to other gas-phase group- and proton-transfer reactions to which we have applied[25] statistical theory (Rice–Ramsperger–Kassel–Marcus theory (RRKM)) for the interpretation of reaction kinetics. This assumption is reasonable considering its similarity to the widely accepted model for electron-transfer reactions in solution.

Also, since the ion–molecule collision complex is presumably long-lived with respect to the time scale for vibrational energy redistribution due to the strong charge–dipole and charge-induced dipole interactions involved, complete energy randomization within

the complex is assumed, as required for application of the statistical treatment. Evidence of statistical behavior in electron-transfer reactions can be found in exothermic electron-transfer reactions where kinetic energy release decreases (while internal excitation increases) as the complexity of the system increases.[8a] Then, within the framework of a double-well potential energy surface, the statistical model based on RRKM theory[25] (the quasi-equilibrium theory of mass spectrometry) allows us to extract an activation barrier (actually E_{dif}, see below) from the experimental reaction rate constant.

Given a reaction occurring on a double-well potential energy surface, Figure 1, the reaction efficiency will be largely determined by (except when the reaction is only slightly exothermic) the branching fraction, BF = $k_2/(k_{-1} + k_2)$, of the reactant complex, C_R, between the formation of the product complex, C_P (a reactive collision), and the regeneration of the original reactants (an unreactive collision). The former channel is characterized by a tight transition state and the latter by a loose transition state (vide infra). If the overall reaction is sufficiently exothermic (> ca. 2 kcal/mol), C_P will usually generate the final products rather than recross the central barrier and regenerate C_R, the latter channel being entropically unfavorable. Thus, the overall reaction efficiency can be approximated by the branching fraction at which C_R crosses the central barrier and forms C_P. If the reaction is thermoneutral, the branching behaviors of C_R and C_P are identical and the overall reaction efficiency is related to the branching fraction of C_R by eq 3. If the reaction is only slightly exothermic, C_P will recross

$$\text{efficiency} = \frac{\text{BF}}{1 + \text{BF}} \quad \text{thermoneutral reactions} \quad (3)$$

the barrier to regenerate C_R, but its behavior is not symmetric with that of C_R. Thus, the reaction efficiency will be intermediate between BF and that predicted by eq 3. A more complicated expression, eq 4, must be employed for such a case. However,

$$\text{efficiency} = \frac{k_2 k_3}{(k_{-1} + k_2)k_3 + k_{-2}k_{-1}} \quad (4)$$

the only such case in our series of reactions has $\Delta E°_{rxn} = 0.8$ kcal/mol and a very fast reaction rate. A lower limit on $|E_{dif}|$ obtained by approximating the reaction efficiency with BF has practically erased the barrier from the reaction coordinate. A complete analysis using eq 4 was not performed since it was not expected to provide any more information than we can get from the approximate treatment. Because of the unfavorable entropy of formation of the tight transition state, a barrier below the entrance channel (i.e., the tight transition state is energetically more stable than the separated reactants) can still significantly reduce the reaction efficiency.

In terms of RRKM theory, the branching fraction of C_R at a given energy E above the entrance channel is defined by eq 5 (note that E_{dif} is a negative quantity for reactions proceeding at measurable rates), where G_{ET} and G_{ORB} are the sums of states of the electron transfer and orbiting transition states at the energies specified, respectively. Convolution of the chemical activation

$$\text{BF}(E) = \frac{k_2(E - E_{dif})}{k_{-1}(E) + k_2(E - E_{dif})} = \frac{G_{ET}(E - E_{dif})}{G_{ORB}(E) + G_{ET}(E - E_{dif})} \quad (5)$$

energy distribution function[25] at a given temperature T, eq 6a, into BF(E) followed by integration over energy, eq 6b, gives the canonical branching fraction, BF(T), which we can equate with the experimental branching fraction. In eq 6a, E_0 is the energy of the orbiting transition state with respect to C_R, both in their ground states.

$$F(E,T) = \frac{G_{ORB}(E) \exp[-(E + E_0)/kT]}{\int_0^\infty G_{ORB}(E) \exp[-(E + E_0)/kT] \, dE} \quad (6a)$$

$$\text{BF}(T) = \int_0^\infty \text{BF}(E) \, F(E,T) \, dE \quad (6b)$$

(23) (a) Compton, R. N.; Christophorou, L. G.; Hurst, G. S.; Reinhardt, P. W. *J. Chem. Phys.* **1966**, *45*, 4634. (b) Christophorou, L. G. *Adv. Electron. Electron Phys.* **1978**, *46*, 55.

(24) (a) Albery, W. J. *Annu. Rev. Phys. Chem.* **1980**, *31*, 227. (b) Sutin, N. *Prog. Inorg. Chem.* **1982**, *30*, 441. (c) Sutin, N. *Acc. Chem. Res.* **1982**, *15*, 275. (d) Sutin, N.; Brunschwig, B. S. In *Mechanistic Aspects of Inorganic Reactions*; ACS Symposium Series; Rorabacher, D. B., Endicott, J. F., Eds.; American Chemical Society: Washington, DC, 1982; p 105.

(25) (a) Robinson, P. J.; Holbrook, K. A. *Unimolecular Reactions*; Wiley-Interscience: New York, 1972. (b) Forst, W. *Theory of Unimolecular Reactions*; Academic Press: New York, 1973.

Electron-Transfer Reactions between Nitrobenzenes

J. Am. Chem. Soc., Vol. 114, No. 3, 1992 891

BF(T) can then be calculated for different E_{dif} values, and the experimental reaction efficiency, or the corresponding BF, determines the "experimental" E_{dif} which reproduces the experiment.

Molecular parameters, moments of inertia, and oscillator frequencies for the two transition states are needed for numerical calculations of the sums of states in eq 5. Experimental information on the actual transition-state parameters is absent, and we made estimations for the necessary molecular parameters on the basis of our previous experience with other systems. The modeling of the two transitions states is described in the following.

Loose Orbiting Transition State. The orbiting transition state leading from C_R to the regeneration of the reactants is characterized by the centrifugal potential energy barrier and consists of two freely tumbling molecular moieties. They correspond approximately to the unperturbed electron donor (radical anion) and the electron acceptor (neutral molecule) at a separation of 7.3–7.7 Å, determined by the polarizability of the neutral molecule. The oscillator frequencies and moments of inertia of the fragments are also approximated by those of the corresponding unperturbed species. The only exceptions are the original three-dimensional free rotations in the separated reactants. The statistical mechanical expression for the partition function pertaining to the loose transition state has the form as if the rotations of the fragments around the intermolecular axis are coupled to form two one-dimensional rotors. One is an internal rotation and the other is an external rotation about this axis,[26] and the remainder are two two-dimensional free rotors (approximately around the axes perpendicular to the intermolecular axis). The external one-dimensional rotation remains in the tight transition state leading to electron transfer, and they largely cancel in the expression for the branching fraction of C_R. The methodology has been documented elsewhere.[26]

Tight Electron-Transfer Transition State. At the isoenergetic configuration,[24a] the electron donor and acceptor are assumed to be in a parallel geometry[27] with the line connecting the centers of mass of the fragments perpendicular to the benzene ring and at a separation of[28] 4 Å. The close proximity of the fragments freezes the free rotations of the two two-dimensional rotors present in the loose transition state which become (four) hindered librations, and their oscillation frequencies are taken to be 200 cm⁻¹, a value typically found in librational motions of aromatic molecules. This frequency is expected to be only slightly dependent on the masses of the fragments involved if the intermolecular interactions are assumed to be insensitive to substitution. The tight transition state can no longer be approximated as composed of an unperturbed electron donor and acceptor pair at a shorter separation. Instead, its wave functions are best described as a linear combination of those of the electron donor and acceptor and therefore a charge delocalized species due to the isoenergetic character of the transition state. This can easily be understood if one considers a degenerate reaction where the tight transition state must be symmetric with respect to the reactants and products (microscopic reversibility), and therefore, the electron to be transferred can be found in either fragment with equal probability. Consequently, the other frequencies are approximated by taking the geometric mean of the corresponding frequencies of the anion and neutral.

The vibrational frequencies of the neutrals have mostly been assigned, and those for the anions are derived from the neutral
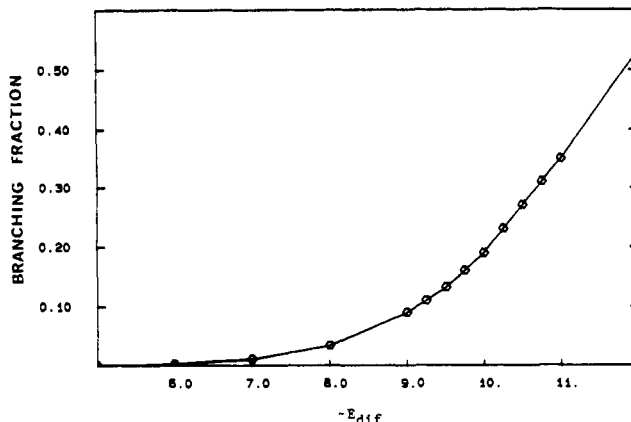

Figure 2. Calculated branching fraction for $NB^{-/0}$ as a function of $-E_{dif}$ (kcal/mol).

frequencies by making proportional changes based on the change in frequencies from neutral[29] $C_6H_5NO_2$ to its radical anion.[30] Local vibrational modes involving the C–N bond, whose π-character is enhanced in the anion, are consistently higher in the anion than in the neutral molecule.

The vibrational modes of the system are various linear combinations of the vibrations of the individual moieties. The reaction coordinate is one of the combinations of ring distortion modes which places both of the moieties (anion and neutral) in identical geometries.

The RRKM reaction efficiency calculation was performed with the direct count algorithm of Hase and Bunker[31] for the sums of states of the loose transition state up to 20 kcal/mol above the entrance channel and of the tight transition state for the first 10 kcal/mol followed by the Whitten–Rabinovitch semiclassical technique for the remaining 10 kcal/mol. At the ICR cell temperature of 350 K, almost all the colliding ion–molecule pairs have a total thermal energy below 20 kcal/mol. The calculated canonical reaction branching fraction, BF(350 K), with an ensemble of microcanonical branching fraction BF(E) at $E \le 20$ kcal/mol is sufficiently accurate and differs by less than 1% from that calculated up to 30 kcal/mol. The calculations included adiabatic rotations but not anharmonicity corrections.

The calculated functional dependence of branching fraction on E_{dif} for the degenerate reaction $NB^{-/0}$ is shown in Figure 2. From the experimental reaction efficiency of 0.14–0.19, the branching fraction (BF) is calculated, using eq 5, to be 0.16–0.24. This range of branching fraction is obtained when E_{dif} has a value of 10.1 ± 0.4 kcal/mol. E_{dif} values determined from RRKM simulations of the experimental reaction efficiencies for five systems are listed in Table I.

Intersecting Parabolas Model. Barriers to electron transfer are frequently analyzed in the framework of Marcus theory and the intersecting parabolas model.[24] In this treatment, the adiabatic barrier in an identity electron-transfer reaction in the absence of electronic coupling[32,33] can be shown to be equal to one-fourth of the energy required to distort the anion to the geometry of the neutral. We carried out MNDO calculations[34] on the neutral nitrobenzene and 3-chloronitrobenzene and their respective radical anions. The geometries were optimized for the neutrals and the

(26) (a) Pellerite, M. J.; Brauman, J. I. *J. Am. Chem. Soc.* **1980**, *102*, 5993. (b) Pellerite, M. J. Ph.D. Thesis, Stanford University, Stanford, CA, 1981.

(27) The parallel conformation is favored in both charge-transfer complexes, see ref 20, and dimers of aromatic molecules; see: Law, K. S.; Schauer, M.; Bernstein, E. R. *J. Chem. Phys.* **1974**, *81*, 4871.

(28) Aromatic charge-transfer complexes typically have separations of 3–4 Å. See: (a) Powell, H. M. *Nature* **1939**, 77. (b) Powell, H. M.; Huse, G.; Cooke, P. W. *J. Chem. Soc.* **1943**, 153. (c) Powell, H. M.; Huse, G.; Cooke, P. W. *J. Chem. Soc.* **1943**, 435. (d) Hagopian, S.; Singler, L. A. *J. Am. Chem. Soc.* **1985**, *107*, 1874. Due to the addition of an extra electron into a pair of closed-shell neutral molecules in the current systems, a separation of 4 Å is assumed. The results of the RRKM modeling do not differ significantly when 3.5 Å is assumed if all the other parameters are fixed.

(29) Laposa, J. D. *Spectrochim. Acta, Part A* **1979**, *35*, 65.

(30) (a) Baronetskii, A. O.; Kuz'yants, G. M. *Izv. Akad. Nauk SSSR, Ser. Khim.* **1980**, 1785. (b) Baronetskii, A. O.; Kuz'yants, G. M. *Bull. Acad. Sci., USSR, Div. Chem. Sci. (Engl. Transl.)* **1981**, 1267.

(31) Hase, W. L.; Bunker, D. L. Quantum Chemistry Program Exchange, No. 234, Indiana University.

(32) In current adiabatic electron-transfer theory, the energy of the transition state is lowered from the zero-order transition state through electronic coupling. Generally, this energy lowering is treated as negligibly small compared to the thermal activation energy. For example, see ref 23c,d.

(33) Cannon, R. D. *Electron Transfer Reactions*; Butterworths: London, 1980.

(34) Thiel, W. Quantum Chemistry Program Exchange, No. 353, Indiana University.

anions, and the energies for the anions were calculated also at the equilibrium geometry of the neutrals. In spite of the problems of accuracy associated with such semiempirical procedures,[35,36] we expect most of the errors to cancel in calculating the distortion energy. We find the vertical distortion energy to be 7.6 and 7.2 kcal/mol for the nitrobenzene and 3-chloronitrobenzene anions, respectively, suggesting barriers to electron transfer in the identity reactions of about 2 kcal/mol in the absence of electronic coupling.

These numbers are of comparable magnitude to the modest barriers (3–5 kcal/mol) derived for the degenerate reactions in Table I. Reactions involving transfer from FNB⁻ to 3-ClFNB, however, (last two entries) are faster than expected if their intrinsic barriers are the same as those for NB⁻/NB⁰. This suggests that the zero-order potential energy surface (which neglects electronic coupling) is not adequate to describe reactions involving halogen substitution on both reactants. Inclusion of electronic coupling is expected to lower the central barrier, thus increasing the rate of reaction.

Electronic coupling matrix elements are needed to construct the first-order potential energy surfaces. These matrix elements are typically 10^2–10^3 cm⁻¹ for adiabatic electron-transfer reactions between inorganic complex ions.[24c,d] This magnitude is enough to account for the discrepancy between the theoretical prediction and the experimental observation for the FNB⁻/3-ClNB reactions.

Rate–Equilibrium Relationship. The Reformulated Marcus Formalism. The Marcus equation,[37] eq 7, has been shown to provide insight into chemical reactivity of gas-phase ion–molecule reactions.[38] The use of eq 7 demands knowledge of the stability

$$\Delta E^* = \Delta E^*_0 + \frac{\Delta E^\circ}{2} + \frac{(\Delta E^\circ)^2}{16\Delta E^*_0} \qquad (7)$$

of the complex ions with respect to the reactants (i.e., E_W) in order to convert E_{dif}, obtained from RRKM calculation of experimental reaction efficiency, into activation energy. However, ion–neutral interaction energies are frequently unavailable, and even if they are, the use of accurate well depths on a case by case basis can be misleading in applying Marcus theory, because the complexes may have stabilization not present in the reactants and/or in the transition state.[39] We therefore rewrite the Marcus equation by defining the reactant as the separated ion and neutral pair and obtain the modified form of the Marcus equation,[39] eq 8.

$$E_{dif} = E^\circ_{dif} + \frac{\Delta E^\circ_{rxn}}{2} + \frac{(\Delta E^\circ_{rxn})^2}{16(E^\circ_{dif} - E_W)} \qquad (8)$$

In eq 8 both E_{dif} and E_W are defined as negative quantities if the corresponding species, the tight transition state and the ion-molecule complex, respectively, are lower in energy than the reactant. Similar to the original Marcus formalism, eq 8 is applicable over a range of reaction energy change given by $|\Delta E^\circ_{rxn}| \leq 4(E^\circ_{dif} - E_W)$. Within this range of reaction exothermicity, the energy barrier decreases monotonically with increasing exothermicity. Equation 8 provides the additional advantage that the overall reaction energy change, ΔE°_{rxn}, rather than the complex-to-complex energy change, ΔE°, is involved. In some of the reactions we studied, the well depths corresponding to C_R and C_P are likely to be significantly different due to the different dipole

moments of the neutral molecules involved in them. Therefore, ΔE° is not, in general, identical to ΔE°_{rxn}, and ΔE° is generally unknown.

In order to apply eq 8 to the kinetic data, we first consider the energy of the ion–molecule complex relative to the reactant. E_W's have not been directly measured for the reaction pairs reported here. Binding energies between SF₆⁻, Cl⁻, NO₂⁻, and some substituted nitrobenzenes have been measured by high-pressure mass spectrometry.[40] Most binding energies fall between ca. 15 and 20 kcal/mol. Since the XNB⁻ are charge-delocalized species, the ion–neutral interactions are expected to be lower than those involving small ions. Therefore, we assumed a lower and nearly constant value of 15–16 kcal/mol for the ion–neutral binding energy or $-E_W$ for the reactions studied. In degenerate systems there may be additional stabilization of the ion–neutral complex due to resonance effects.[41,42]

If the well depth, $-E_W$, is as large as 15 kcal/mol, then the MNDO calculated barrier of ca. 2 kcal/mol gives an E_{dif} of ca. 13 kcal/mol. Considering the assumptions in the statistical treatment, the quantum calculations, and the estimate of the well depth, the agreement is quite satisfactory.

From the results for the two degenerate reactions summarized in Table I, we find that although the rates are similar, the intrinsic activation energies, measured by E°_{dif}, are not identical. The source of the different E°_{dif}'s obtained from the statistical model for the two degenerate reactions can be attributed to different molecular properties of the reactants involved, including changes in moments of inertia and symmetry and ion–neutral binding energies between the two degenerate systems.

Alternatively, the difference in E_{dif} may be a consequence of the assumptions made in the statistical treatment. For example, we have fixed the librational frequencies of the electron-transfer transition states to be 200 cm⁻¹ in all reactions. This is equivalent to assuming a constant intermolecular interaction in all the tight transition states. While the nature of the tight transition states may be actually different in different reactions, adjustment of transition-state parameters in the absence of experimental librational frequencies is not justified in a quantitative analysis, because a range of E_{dif} can be obtained by adjusting the transition-state parameters. Although the kinetics suggest a small difference in E_{dif} while the MNDO calculations do not, the overall agreement is remarkably good in view of the assumptions involved.

The results in Table I also indicate acceleration of reaction by thermodynamic driving force as one would have expected from rate–equilibrium relationships. Although the nonconstant E°_{dif} obtained for the two degenerate reactions introduces some error into a quantitative test of rate–equilibrium relationships by applying eq 8, the results are quite consistent with those predicted by eq 8. The acceleration in reaction rates, however, appears to be extraordinarily large between the two FNB⁻/3-ClNB pairs (last two entries in Table I). It suggests the involvement of additional electronic coupling when halogen substituents are present in both the electron donor and acceptor or when they both form more stable parent radical anions than NB⁻. This behavior of halogenated NB is consistent with the lower E°_{dif} obtained for 3-ClNB⁻/⁰ than that for NB⁻/⁰.

Conclusion

Our results suggest that the statistical model may be appropriate for analyzing electron-transfer reactions of this type. The observed acceleration of rates with increasing thermodynamic driving force is in good agreement with predictions based on Marcus theory.

(35) (a) Dewar, M. J. S.; Thiel, W. *J. Am. Chem. Soc.* **1977**, *99*, 4907. (b) Dewar, M. J. S.; Ford, G. P. *J. Am. Chem. Soc.* **1979**, *101*, 5558. (c) Carrion, F.; Dewar, M. J. S. *J. Am. Chem. Soc.* **1984**, *106*, 3531. (d) Dewar, M. J. S.; Storch, D. M. *J. Am. Chem. Soc.* **1985**, *107*, 3898. (e) Dewar, M. J. S.; Zoebisch, E. G.; Healy, E. F.; Stewart, J. J. P. *J. Am. Chem. Soc.* **1985**, *107*, 3902.

(36) It is necessary to include diffuse orbitals in ab initio calculations for anions, and the calculated anion energies are commonly less accurate than those obtained for cations and neutral molecules. See, for example: Latajka, Z.; Scheiner, S. *Int. J. Quantum Chem.* **1986**, *29*, 285. Lee, T. J.; Schaefer, H. F., III. *J. Chem. Phys.* **1985**, *83*, 1784.

(37) Marcus, R. A. *J. Phys. Chem.* **1968**, *72*, 891.

(38) Pellerite, M. J.; Brauman, J. I. *J. Am. Chem. Soc.* **1983**, *105*, 2672.

(39) Dodd, J. A.; Brauman, J. I. *J. Phys. Chem.* **1986**, *90*, 3559.

(40) (a) Chowdhury, S.; Kebarle, P. *J. Chem. Phys.* **1986**, *85*, 4989. (b) Grimsrud, E. P.; Chowdhury, S.; Kebarle, P. *Int. J. Mass Spectrom. Ion Processes* **1986**, *68*, 57.

(41) In the symmetric dimer anion of toluquinone, which corresponds to the intermediate complex ion formed in the corresponding degenerate electron-transfer reaction, the extent of electron delocalization was determined to be only 5–10%. See ref 42c.

(42) (a) Meot-Net, M. *J. Phys. Chem.* **1980**, *84*, 2724. (b) Jarrold, M. F.; Illies, A. J.; Wagner-Redeker, W.; Bowers, M. T. *J. Phys. Chem.* **1985**, *89*, 3269. (c) Comita, P. B.; Brauman, J. I. *J. Am. Chem. Soc.* **1987**, *109*, 7591.

The intersecting parabolas model predicts a barrier consistent with that of the statistical treatment. Quantitative deviations suggest that electronic coupling may prove to be important in understanding the barrier heights.

Complete Conversion of L-Lactate into D-Lactate. A Generic Approach Involving Enzymatic Catalysis, Electrochemical Oxidation of NADH, and Electrochemical Reduction of Pyruvate

Azz-Eddine Biade,[1] Christian Bourdillon,[2] Jean-Marc Laval,[2] Gilles Mairesse,[1] and Jacques Moiroux*

Contribution from the Laboratoire d'Electrochimie Moléculaire de l'Université Paris 7, Unité de Recherche Associée au CNRS No. 438, 2 place Jussieu, 75251 Paris Cedex 05, France. Received July 25, 1991

Abstract: L-Lactate was converted into D-lactate with a yield better than 97%, the system involving stereospecific catalysis of L-lactate oxidation by the rather cheap L-lactate dehydrogenase plus electrochemical regeneration of NAD^+ at the anode and electrochemical reduction of pyruvate at the cathode. Such an approach can be extended to mere deracemization or complete inversion of all types of chiral α-alcohol–acids provided that the dehydrogenase related to the isomer to be inverted is available. Efficiency was not limited by enzyme or coenzyme deactivations.

The abilities of enzymes to discriminate between enantiomers of racemic substrates are outstanding, and multiple ways of exploiting these enantiomeric specificities have been investigated with the purpose of developing processes for the preparation of chiral compounds.[3]

Resolution of racemic mixtures via acylase[4] or lipase[5] catalyses of α-functionalized carboxylates are well documented. Acylase mediated resolutions of N-acyl amino acids are industrially important.[4b] They proceed according to the following reaction sequence: first, the L-enantiomer is catalytically transformed into the L-amino acid; second, the unhydrolyzed N-acyl D-amino acid is recycled via chemically induced racemization.

Dehydrogenases are also potentially useful catalysts in chiral synthesis.[6,7] Oxidation of a chiral alcohol or amine is stereospecific, but the net result of such a transformation is most often the loss of chirality since it produces a carbonyl compound with concomitant disappearance of the initial asymmetry of the carbon atom bearing the hydroxy or amino substituent. There are only

few examples in which the production of the carbonyl group can create a new asymmetry as may occur when preparing D-glyceraldehyde by means of enzymatic (glycerol dehydrogenase, E.C. 1.1.1.72. plus $NADP^+$) oxidation of glycerol. Therefore, the reductive transformation of a pro-chiral carbonyl compound into an alcohol or an amine is of much greater interest as long as the aim is the production of chiral species and, generally, it is a thermodynamically favorable reaction. Most of the dehydrogenases are NAD(P)(H)-requiring oxidoreductases[8] although there exist some important exceptions.[8b,9] Enzymatic regeneration of NAD(P)H from $NAD(P)^+$ is now relatively straightforward.[7,8,10] Chemical redox mediation of the electrochemical regeneration is also possible.[11] Inherently, these two methods imply either the introduction in the medium of a second enzyme and a second substrate, or at least a chemical redox mediator. Moreover, the enzyme-catalyzed reduction of a prochiral carbonyl derivative on a preparative scale has a built-in disadvantage when aiming at the production of the less naturally occurring enantiomer since the related enzyme, if available, is usually rather expensive.

(1) Laboratoire d'Electrochimie des Substrats Enzymatiques, Faculté de Pharmacie, Université de Picardie, 1 rue des Louvels, 80037 Amiens Cedex 1, France.
(2) Laboratoire de Technologie Enzymatique, Unité de Recherche Associée au CNRS No. 1442, Université Technologie de Compiègne, BP 649, 60206 Compiègne Cedex, France.
(3) Review: Jones, J. B. *Tetrahedron* 1986, *42*, 3351.
(4) (a) Greinstein, J. P. *Adv. Protein Chem.* 1954, *9*, 122. (b) Chibata, I.; Tosa, T.; Sato, T.; Mori, T. *Methods Enzymol.* 1976, *44*, 746.
(5) Kirchmer, G.; Scollar, M. P.; Klibanov, A. M. *J. Am. Chem. Soc.* 1985, *107*, 7072 and references therein.
(6) Reviews: (a) Jones, J. B. *Asymmetric Synthesis*; Morrison, J. D., Ed.; Academic Press: New York, 1985. (b) Whitesides, G. M.; Wong, C. H. *Aldrichimica Acta* 1983, *16*, 27.
(7) (a) Hirschbein, B. L.; Whitesides, G. M. *J. Am. Chem. Soc.* 1982, *104*, 4458. (b) Wandrey, C.; Buckmann, A. F.; Kula, M. R. *Biotechnol. Bioeng.* 1981, *23*, 2789.

(8) Reviews: (a) Hummel, W.; Kula, M. R. *Eur. J. Biochem.* 1989, *184*, 1. (b) Simon, H.; Bader, J.; Günther, H.; Neumann, S.; Thanos, J. *Angew. Chem., Int. Ed. Engl.* 1985, *24*, 539.
(9) Skopan, H.; Günther, H.; Simon, H. *Angew. Chem., Int. Ed. Engl.* 1987, *26*, 128.
(10) (a) Shaked, Z.; Whitesides, G. M. *J. Am. Chem. Soc.* 1980, *102*, 7104. (b) Vandercasteele, J. P.; Lemal, J. *Bull. Soc. Chim. Fr.* 1980, 101. (c) Wong, C. H.; Drueckhammer, D. G.; Sweers, H. M. *J. Am. Chem. Soc.* 1985, *107*, 4028. (d) Matounaga, T.; Matounaga, N.; Nishimura, S. *Biotechnol. Bioeng.* 1985, *27*, 1277. (e) Ohshima, T.; Wandrey, C.; Conrad, D. *Biotechnol. Bioeng.* 1989, *34*, 394. (f) Parson, M.; Mansson, M. O.; Bulow, L.; Mosbach, K. *Bio/Technology* 1991, *9*, 280.
(11) Ruppert, R.; Herrmann, S.; Steckhan, E. *Tetrahedron Lett.* 1987, *28*, 6583.